Proc. Natl. Acad. Sci. USA
Vol. 95, pp. 10564–10569, September 1998
Biophysics

Structure of *Fok*I has implications for DNA cleavage

DAVID A. WAH*, JURATE BITINAITE†, IRA SCHILDKRAUT†, AND ANEEL K. AGGARWAL*‡

*Structural Biology Program, Department of Physiology and Biophysics, Box 1677, 1425 Madison Avenue, Mount Sinai School of Medicine, New York, NY 10029; and †New England Biolabs, 32 Tozer Road, Beverly, MA 01915

Edited by Robert T. Sauer, Massachusetts Institute of Technology, Cambridge, MA, and approved June 22, 1998 (received for review April 7, 1998)

ABSTRACT ***Fok*I is a member an unusual class of restriction enzymes that recognize a specific DNA sequence and cleave nonspecifically a short distance away from that sequence. *Fok*I consists of an N-terminal DNA recognition domain and a C-terminal cleavage domain. The bipartite nature of *Fok*I has led to the development of artificial enzymes with novel specificities. We have solved the structure of *Fok*I to 2.3 Å resolution. The structure reveals a dimer, in which the dimerization interface is mediated by the cleavage domain. Each monomer has an overall conformation similar to that found in the *Fok*I–DNA complex, with the cleavage domain packing alongside the DNA recognition domain. In corroboration with the cleavage data presented in the accompanying paper in this issue of *Proceedings*, we propose a model for *Fok*I DNA cleavage that requires the dimerization of *Fok*I on DNA to cleave both DNA strands.**

*Fok*I, from *Flavobacterium okeanokoites*, is a member of the unusual, type IIs class of restriction endonucleases that recognize a specific DNA sequence and cleave nonspecifically a short distance away from that sequence (1). *Fok*I binds the cognate sequence 5′-GGATG-3′ and cleaves DNA phosphodiester groups 9 bp away on this strand and 13 bp away on the complementary strand (Fig. 1). *Fok*I has been shown to consist of two functionally distinct domains: an N-terminal DNA recognition domain and a C-terminal DNA cleavage domain (2). The modular nature of *Fok*I has led to the development of artificial enzymes with new specificities (3–7).

We recently reported the structure of *Fok*I bound to a 20-bp DNA fragment containing the *Fok*I cognate sequence (8). As expected, the protein has N- and C-terminal domains corresponding to the DNA recognition and cleavage functions, respectively. The recognition domain is comprised of three smaller subdomains (D1, D2, and D3) that are evolutionarily related to the helix-turn-helix- containing DNA-binding domain of the catabolite gene activator protein (9). The catabolite activator protein core has been embellished extensively in D1 and D2, whereas in D3 it has been co-opted for protein–protein interactions. The cleavage domain is similar to a *Bam*HI monomer and contains a single catalytic center, which raises the question of how monomeric *Fok*I manages to cleave both strands. In a novel mechanism of nuclease activation, the recognition domain sequesters the cleavage domain through protein–protein interactions until its activity is required, whereby the cleavage domain dissociates from the recognition domain and swings over to the major groove for DNA cleavage. We have now determined the structure of *Fok*I in the absence of DNA. The structure, determined at 2.3 Å resolution, reveals a dimer, in which the dimerization interface is mediated by the cleavage domain. Each monomer has an overall conformation similar to that found in the *Fok*I–DNA complex, with the cleavage domain packing alongside the DNA recognition domain. In corroboration with the cleavage data presented in the accompanying paper in this issue of *Proceedings* (10), we propose a model for *Fok*I DNA cleavage that requires the dimerization of *Fok*I on DNA to cleave both DNA strands.

EXPERIMENTAL METHODS

Crystallization. *Fok*I was expressed and purified as described (11). Chunky crystals (0.25 mm × 0.25 mm × 0.4 mm) grew in 3–4 days at 20°C from 2 μl of sitting drops containing 0.12 mM protein, 11% polyethylene glycol (average molecular weight 8,000), 0.2 M ammonium sulfate, 50 mM sodium cacodylate (pH 6.5), 0.2 M potassium chloride, 10 mM potassium phosphate, 0.5 mM DTT, 0.5 mM EDTA, 0.5 mM EGTA, and 5% glycerol when equilibrated against a reservoir containing 22% polyethylene glycol 8,000, 0.4 M ammonium sulfate, and 0.1 M sodium cacodylate (pH 6.5). Crystals were stabilized and cryoprotected in 23% polyethylene glycol, 0.4 M ammonium sulfate, 0.1 M sodium cacodylate (pH 6.5), and 15% ethylene glycol. Transient addition of 0.125% glutaraldehyde was necessary to prevent the crystals from shattering.

Data Collection and Structure Determination. The crystal used in data collection diffracted to 2.3 Å resolution when flash-cooled in a nitrogen gas stream at −160°C and exposed to synchrotron radiation. The crystal belongs to space group $P2_12_12_1$ with unit cell dimensions of a = 54.0 Å, b = 137.2 Å, and c = 188.9 Å. Data were measured at the Cornell High Energy Synchrotron Source by using imaging plates on beamline A1 at λ = 0.908 Å. Data were processed with DENZO (12) and reduced with Scalepack and TRUNCATE (13).

The structure of *Fok*I was solved by molecular replacement by using AMORE software (14). The cleavage domain (residues 390–579) from the refined structure of the *Fok*I–DNA complex was used as the initial search model. Rotation and translation functions revealed two molecules per asymmetric unit, consistent with a V_m of 2.7. Assuming that the association between the recognition and cleavage domains seen in the *Fok*I–DNA complex would remain intact in the free enzyme, the full length *Fok*I structure from the refined complex was fit by least-squares with the program O (15) to the two translation solutions for the cleavage domain. Visual inspection of this model revealed unambiguously a dimer in the asymmetric unit, with no steric clashes between the monomers or the symmetry-related molecules. The dimer solution was subjected to rigid body refinement in X-PLOR (16). After a subsequent round of simulated annealing, the *R*-factor dropped to 0.289 with an *R*-free = 0.377. Several rounds of rebuilding, interspersed with positional and simulated annealing refinement, yielded the current model at 2.3 Å resolution. The model was verified through extensive simulated annealing omit maps in which 15 consecutive residues were omitted at a time. Solvent molecules

The publication costs of this article were defrayed in part by page charge payment. This article must therefore be hereby marked "*advertisement*" in accordance with 18 U.S.C. §1734 solely to indicate this fact.

This paper was submitted directly (Track II) to the *Proceedings* office.
Data deposition: The atomic coordinates have been deposited in the Protein Data Bank, Biology Department, Brookhaven National Laboratory, Upton, NY 11973 (PDB ID code 2FOK).

‡To whom reprint requests should be addressed. e-mail: aggarwal@inka.mssm.edu.

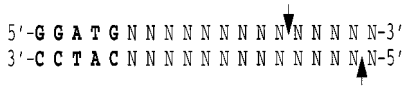

FIG. 1. Recognition sequence of *Fok*I. *Fok*I cleaves phosphodiester groups 9 bp away on the 5′ strand and 13 bp away on the 3′ strand, as indicated by arrows.

(516) were added to the model (B-values < 55 Å^2) from inspection of F_o-F_c maps. Residues A1-A4, A77-A81, A97-A98, A252-A256, A380-A385, B1-B4, B62-B63, B77-B81, and B379-B386 could not be built because of uninterpretable density.

RESULTS AND DISCUSSION

Overall Structure. The structure of *Fok*I was determined at 2.3 Å resolution (Table 1). The crystal contains one dimer per asymmetric unit. A noncrystallographic symmetry axis lies between the cleavage domains and continues up between the D1 subdomains of each monomer (Fig. 2*a*). The secondary structure of each monomer is virtually identical to that found in the *Fok*I–DNA complex (Fig. 2*b*). Subdomain D1 of the recognition domain is comprised of eight helices (α1 to α8), two loops (L1 and L2), a β-sheet (β1 to β3), and an N-terminal arm. The embellished helix-turn-helix motif is made of helices α4, α5, and α6 and loops L1 and L2. The short helices α4 and α5 share the same helical axis, as if they formed a single α-helix into which L1 has been inserted. Together, helices α4 and α5 (α4/5) form the first helix of the helix-turn-helix motif, and α6 is the second helix, also known as the recognition helix. The turn expected between α4/5 and α6 is replaced by L2. D2 is an extended structure of six helices (α1 to α6), a β-sheet (β1, β2, β5), a β-hairpin (β3, β4), and a short loop L1. In this subdomain, the embellished helix-turn-helix motif is comprised of helices α2 and α5. The turn is replaced by loop L1, a pair of antiparallel helices α3 and α4, and a short segment T1 connecting α4 to α5. D3 is most similar to catabolite activator protein, having a three-helix/β-sheet structure. The cleavage domain resembles a subunit of the dimeric endonuclease *Bam*HI (17) and comprises a mixed six-stranded β-sheet (β1 to β6) with α-helices (α1, α2, α3, α6 and α4, α5) on each side.

Comparison with the Structure of the *Fok*I–DNA Complex. Surprisingly, the overall conformation of each *Fok*I monomer is similar to that found in the *Fok*I–DNA complex (Fig. 3). This was unexpected because the *Eco*RV and *Bam*HI structures showed large conformational changes on DNA binding (17–19). However, despite the overall similarity in fold, there are important structural differences between the free and bound forms of *Fok*I. For example, subdomain D1 is pivoted ≈5° away from the DNA-binding cleft, whereas the antiparallel helices α3 and α4 of subdomain D2 are tilted into the cleft. The cleavage domain has moved ≈1 Å toward the recognition domain in a direction parallel to the DNA dyad axis, resulting in a narrowing of the interface between the two domains. The linker segment, which was rigid in the complex, is partially disordered in the free enzyme. In the *Fok*I–DNA complex, subdomain D1 recognized base pairs at the 3′ end of the recognition sequence (GGATG) through the recognition helix α6, the loops L1 and L2, and an N-terminal arm. Of interest, the residues (Arg-79 and Gln-95) in loops L1 and L2 that gripped the DNA in both the major and minor grooves are disordered in the free enzyme, implying that they become ordered only in the presence of DNA. Also, the side-chain of Trp 105 (from helix α6) that made van der Waals contacts with the thymine of the fourth base pair and the cytosine of the fifth base pair (GGATG) in the major groove is flipped out into the solvent. A solvent-exposed tryptophan, although rare, also has been seen in the structure of CD4 (20, 21). In the N-terminal arm, the side-chain of Pro-14 maintains its trans configuration but is also flipped out toward solvent, resulting in a local rearrangement of the adjacent residues. In subdomain D2, which recognizes base pairs at the 5′ end of the recognition sequence (GGATG), the recognition helix α5 maintains the same position in the DNA-binding cleft, while helix α4 has rotated 14° from its DNA-binding position, where it contacted the cytosine of the first base pair. This rotation causes the tilt of the antiparallel helices α3 and α4 toward the DNA-binding cleft in the free enzyme. Taken together, the conformational changes observed in D1 and D2 are sufficient to prevent the docking of DNA to the free enzyme structure without steric clashes.

As in the *Fok*I–DNA complex, the cleavage domains in the *Fok*I dimer pack alongside the recognition domains, sequestered through protein–protein interactions. This is consistent with the mechanism of nuclease activation delineated from the *Fok*I–DNA complex (8) and a study of *Fok*I mutants that cleave hemi-methylated DNA (22). These mutants were shown to contain amino acid substitutions in residues located in the interface between the recognition and cleavage domains (8). Such mutations would be expected to relax the domain–domain association, accelerating the rate of *Fok*I activity to cleave at even hemi-methylated cognate sites (22).

We had suggested that, after *Fok*I binds the cognate site in the presence of Mg^{2+}, the cleavage domain would be activated to dissociate from the recognition domain and swing over to the major groove, one turn away from the recognition sequence. Additional evidence for this mechanism comes from the free enzyme structure. The protein–protein interactions at the interface between the recognition domain and the cleavage domain are maintained in the free enzyme, but the narrowing of the interface results in additional interactions not seen in the complex. These interactions are mediated by water molecules between helix α4 and the turn T1 of subdomain D2 and helix α3 of the cleavage domain. The most significant of these involve Gln-420 and Arg-422 of the cleavage domain, which form solvent mediated hydrogen bonds with the side-chain of Lys-225 and the main-chain carbonyl of Glu-220 of D2, respectively. In the *Fok*I–DNA complex, this water structure is displaced by the DNA sugar–phosphate backbone, and Glu-220 and Lys-225 make base-specific contacts with the DNA. The disruption of the hydrogen-bonding network between the two domains along with the replacement of protein–protein contacts with protein–DNA contacts on specific DNA binding may provide part of the free energy necessary for the cleavage domain to dissociate from the recognition domain to initiate cleavage.

The Dimer Interface. The dimer interface is formed by the parallel helices α4 and α5 and two loops P1 and P2 of the cleavage domain (Fig. 4). The helix α4 of each monomer is roughly perpendicular to helix α4 of the other monomer, and

Table 1. Crystallographic analysis

Data collection statistics	
Space group	$P2_12_12_1$
Resolution, Å	2.3
Unique reflections	61150
Data coverage, %	95.9
R_{merge}*, %	8.2
Refinement statistics	
Resolution range, Å	6-2.3
Reflections, $F > 2\sigma(F)$	57475
R-factor,† %	21.1
R-free,‡ %	30.6
rms bond lengths, Å	0.007
rms bond angles, °	1.2

*$R_{merge} = \Sigma|I_{obs} - \langle I\rangle|/\Sigma\langle I\rangle$
†R-factor $= \Sigma| |F_o| - |F_c| |/\Sigma|F_o|$
‡Calculated with 3% of the reflections omitted from refinement.

a

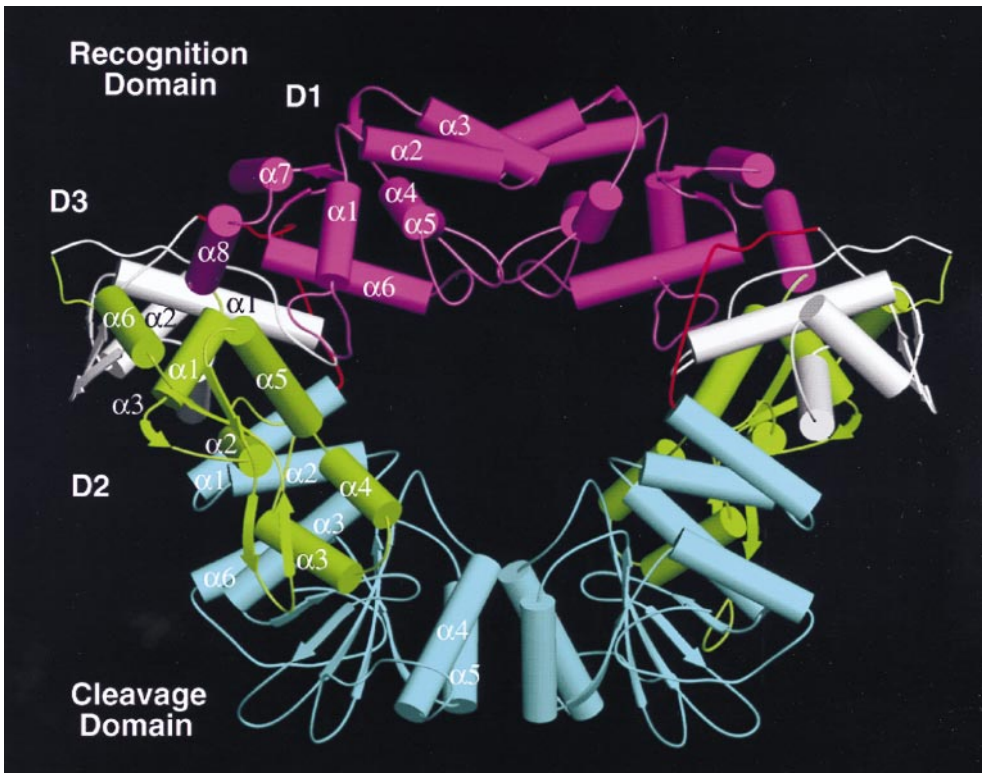

b

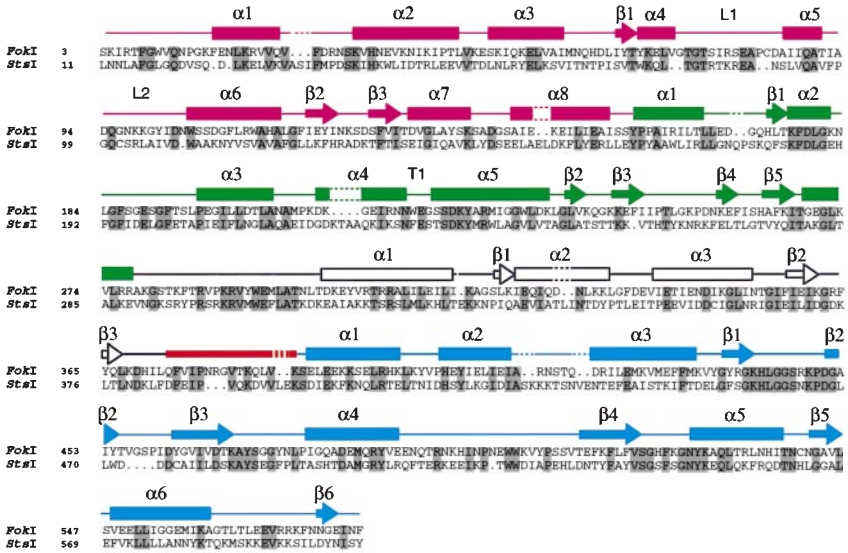

FIG. 2. (*a*) Structure of the *Fok*I dimer. The recognition domain consists of three smaller subdomains, D1, D2, and D3 shown in magenta, green, and white, respectively. The cleavage domain (blue) is connected to the recognition domain through a linker segment (red). Dimerization is mediated by the parallel helices α4 and α5 of the cleavage domain. There are no significant interactions between the D1 subdomains despite the appearance of such in this orientation of the structure. (*b*) Secondary structure assignment of *Fok*I. The *Fok*I amino acid sequence is aligned to that of *Sts*I, another type IIs restriction enzyme. *Sts*I recognizes the same sequence as *Fok*I (Fig. 1) but cleaves 10 and 14 bp away. *Fok*I and *Sts*I show 30% sequence identity (residues in gray columns). Dashes in the secondary structure and periods in the sequence represent gaps introduced for optimal alignment.

together, the two helices make up the core of the dimer interface. The core is sandwiched between the helix α5 and loops P1 and P2 from each monomer, where loop P1 comes between the β-strands β1 and β2 and loop P2 is at the C terminus of α4.

The *Fok*I dimer interface is reminiscent of the dimer interface of *Bam*HI, consisting of a 4-helix bundle formed by the parallel helices α4 and α6 from each subunit (17). The similarity between the helices α4 and α5 in *Fok*I and α4 and α6 in *Bam*HI led us to suggest that *Fok*I might dimerize on DNA. However, in stark contrast to the hydrophobic core found in the *Bam*HI dimer interface, the *Fok*I core is primarily electrostatic with the hydrophobic interactions limited to the edges. These hydrophobic interactions are made through loops P1 and P2. The residue Ile-499 of P2 fits into a hydrophobic pocket formed by Arg-534, His-537, and Ile-538 at the C-

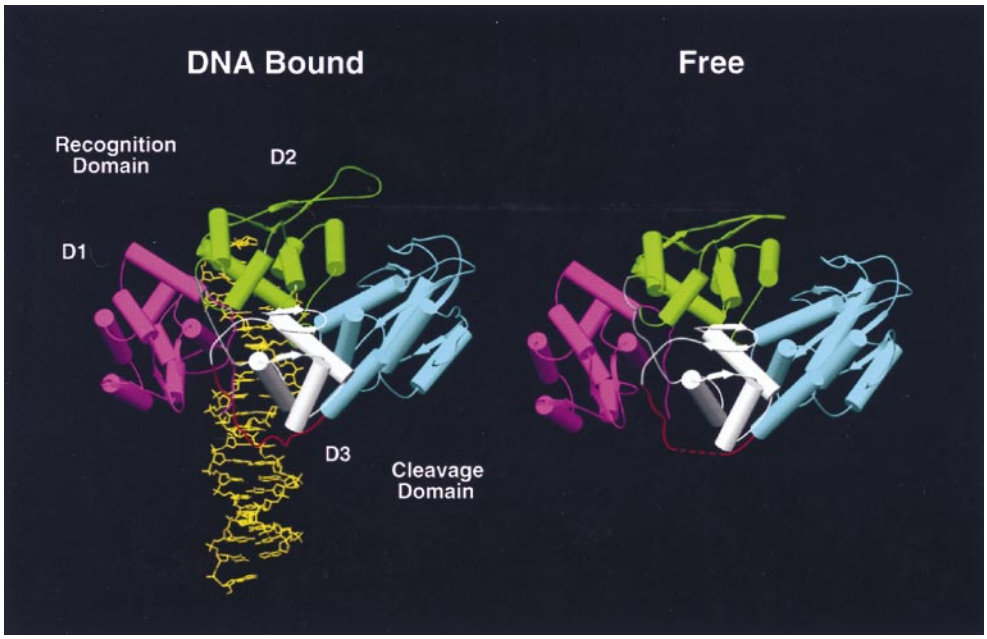

FIG. 3. Comparison of the *Fok*I–DNA complex (8) to a monomer of the *Fok*I dimer. The two structures superimpose with an rms deviation of 1.2 Å using 553 C_α atoms. The linker segment (red dashes) is disordered in the *Fok*I dimer.

terminal end of helix α5 of the other monomer. Ile-479 of α4 makes van der Waals contact with the δ-carbon of Arg-447 of loop P1. Inside the core, the majority of interactions are mediated through an extensive water structure. For example, Arg-534 of α5 makes a water-mediated contact with Glu-491 of α4 of the other monomer. Each of these residues is stabilized through hydrogen bonding to a solvent molecule and another residue from its respective helix. Dimerization may be weakened by the proximity of the two Glu-490 residues from the α4 helices, whose side-chain oxygens are ≈5 Å apart. However, this negative effect is reduced by hydrogen bonding with the adjacent Asn-486 residues. The only direct hydrogen bonding between the monomers occurs at the core of the interface, where Asp-483 from helix α4 makes bidentate hydrogen bonds with Arg-487 from helix α4 of the other monomer (Fig. 4). In accordance with the structure, we show in the accompanying paper (10) that mutation of both residues to alanine causes the loss of cleavage of both strands, suggesting that dimerization of *Fok*I is necessary for cleavage. This dimerization is mediated by the cleavage domains as in our structure. However, the arrangement of the recognition domains in our structure probably does not correspond to the active dimeric form of the enzyme because the modeling of DNA in the DNA-binding cleft of each monomer results in severe steric clashes.

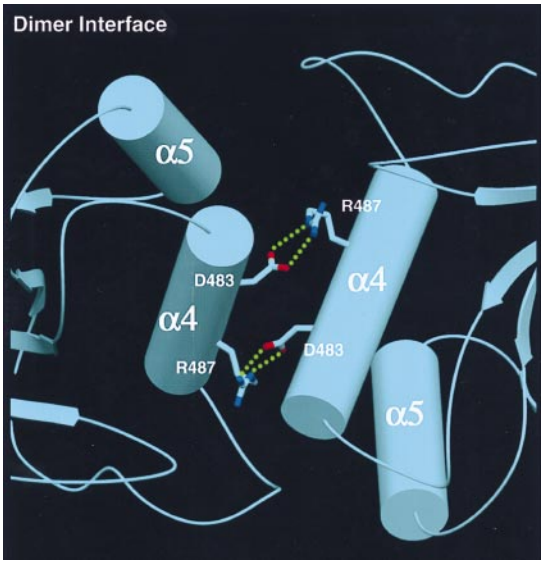

FIG. 4. The *Fok*I dimer interface. Dimerization is mediated primarily through parallel helices α4 and α5 of the cleavage domain. The two α4 helices are roughly perpendicular to each other. The residue Asp-483 of α4 makes bidentate hydrogen bonds with Arg-487 of α4 of the other monomer and *vice versa*. Mutation of both residues eliminates cleavage of both strands [see accompanying paper (10)].

***Fok*I Dimer/DNA Model.** The similarity between *Bam*HI and *Fok*I allowed us to use the structure of the *Ba*mHI–DNA complex (19) to model the *Fok*I cleavage domain dimer onto DNA (Fig. 5). The DNA lies in a cleft created by the cleavage domains, without any steric clashes with the enzyme (Fig. 5). As in *Bam*HI, the N termini of the dimerization helices are directed toward the major groove (19). Both *Bam*HI and *Fok*I make 4-bp staggered cuts, and the residues involved in catalysis [Asp-94, Glu-111, and Glu-113 in *Bam*HI (17) and Asp-450, Asp- 467 and Lys-469 in *Fok*I (23)] overlap at both catalytic sites. The catalytic residues are in close proximity to the phosphodiester bonds that they hydrolyze. In contrast to *Bam*HI, there are no residues that could make base-specific contacts with the DNA (19). This is not surprising because the *Fok*I cleavage domain demonstrates no DNA-binding specificity (2). However, the dipole moments of the dimerization helices should contribute electrostatically to the stabilization of the cleavage complex (24).

Similarity Between *Fok*I and *Sts*I. The structure of *Fok*I provides the first view of a member of the growing family of type IIs restriction endonucleases (25). Based on the structure of *Fok*I, we predict that another type IIs restriction endonuclease *Sts*I would have a bipartite structure similar to *Fok*I. *Sts*I recognizes the same cognate site, GGATG, as *Fok*I, but cleaves 10 and 14 bp away (26). *Sts*I and *Fok*I share 30% sequence identity (27), and their sequences can be aligned as shown in Fig. 2*b*. From the alignment, it is clear that all of the active site and almost all of the DNA recognition residues are conserved between the two proteins. For instance, Trp-105 of *Fok*I, which makes van der Waals interactions in the major groove of the recognition sequence, aligns with Trp-109 in *Sts*I. Also, Arg-79 of *Fok*I aligns with Lys-86 of *Sts*I, and like Arg-

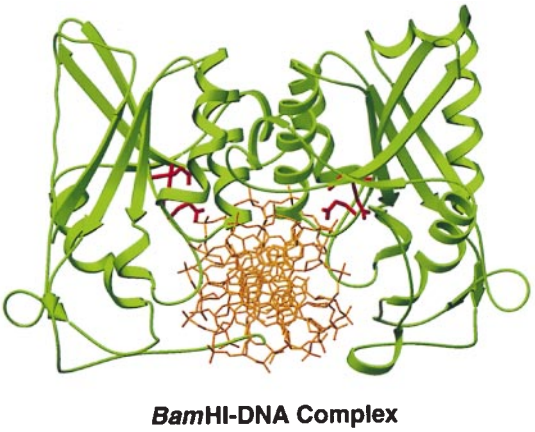

FIG. 5. Comparison of the *Bam*HI–DNA complex (18) with a model of the cleavage domain dimer bound to the *Fok*I cleavage site. Active site residues Asp-94, Glu-111, and Glu-113 in *Bam*HI and Asp-450, Asp-467, and Lys-469 in *Fok*I are in red. In both structures, the dimerization helices point into the major groove and are roughly perpendicular to it. The *Fok*I dimer provides a prominent cleft for the DNA with the two active sites in close proximity to the scissile bonds.

79, this lysine also could make similar contacts to the guanine of the fifth base pair. Similarly, Gln-12 and Asn-13 of *Fok*I, which recognize the two adenine bases, align with Gln-20 and Asp-21 of *Sts*I. Although Asp-21 would not be able to maintain the bidentate hydrogen bonding pattern that Asn-13 has to the O6 and N7 of adenine, it could form a single hydrogen bond to just N7. Taken together, the structure of *Fok*I helps to identify the plausible DNA recognition residues of *Sts*I and provides a basis for understanding how the two enzymes recognize the same DNA site.

An interesting question in comparing *Sts*I and *Fok*I relates to the difference in cleavage distance. A simple view would be that the *Sts*I linker segment is longer to allow cleavage 10 and 14 bp away. However, our alignment shows that this is not the case because the linker segment and helices α1 and α2 of the cleavage domains of the two enzymes align well. On the other hand, *Sts*I has four extra residues in the loop between helices α2 and α3 of the cleavage domain (Fig. 2*b*). The loop is predicted to interact with the DNA backbone when the cleavage domain swings over for catalysis. The fact that some of these extra residues are lysines may affect the way in which the cleavage domain of *Sts*I docks onto the DNA, placing it 1 bp further along the DNA backbone.

DNA Cleavage by *Fok*I. How does *Fok*I cleave DNA? In the accompanying paper (10), we show that, in the presence of excess *Fok*I cognate sites, *Fok*I cleaves DNA at a rate higher

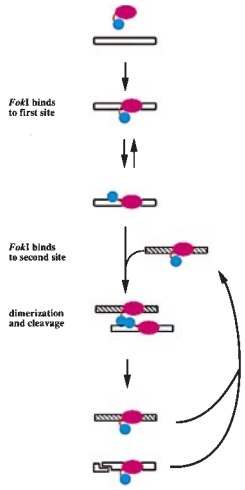

FIG. 6. A model of *Fok*I cleavage. First, a *Fok*I monomer binds DNA at its recognition site. Upon binding and in the presence of Mg^{2+}, the cleavage domain dissociates from the recognition domain. A second *Fok*I molecule, bound to another recognition site, dimerizes with the first molecule through their cleavage domains and catalyzes cleavage at the first site. After cleavage, the two *Fok*I molecules dissociate from the DNA or they remain bound and catalyze additional cleavages by dimerizing with *Fok*I molecules bound to other sites.

than first order, suggesting that the enzyme works as a dimer. Our structure indicates that dimerization is mediated through the cleavage domain. Thus, one *Fok*I molecule binds to the cognate site and recruits another *Fok*I molecule, which supplies the second catalytic center through its cleavage domain. In this mechanism, the cleavage domain of the first molecule would be activated on specific DNA binding and swing into an open conformation for dimerization and cleavage. The first molecule is likely to cleave at the scissile bond 13 bp away because the cleavage domain can be brought there by simple rotations around the linker segment, whereas placement at the scissile bond 9 bp away (N9) would require partial unfolding of either D3 or the cleavage domain. Thus, the second molecule is likely to supply the cleavage domain for cleavage at N9 after dimerization.

From our modeling of the cleavage domain at N13, we expect residues 383–387 in the linker segment to dissociate from subdomain D3 and become α-helical. The observed disorder of residues 380–386 in the linker segment of the free enzyme indicates that the linker can dissociate from D3. At the same time, residues 382–384 in the *Fok*I–DNA complex were found to have a slight 3_{10} helical character. Under these conditions, the first helix of the cleavage domain α1 would be extended by 5 residues, acting as a 17-residue helical measuring rod to place the cleavage domain at the correct scissile bond 13 bp away. Chandrasegaran and colleagues (28) have designed a *Fok*I mutant that cleaves 14 bp away by inserting repeats of the residues 387–390 and 387–393. The residues chosen reside at the junction between the linker segment and α1 of the cleavage domain and may have the effect of extending the measuring rod.

The total surface area buried in the *Fok*I dimerization interface in our crystals is only 800 Å^2, well below the value for typical oligomeric proteins (29). This explains why *Fok*I exists as a monomer in solution and only it dimerizes on DNA, with the weak dimerization interface contributing to the cooperativity of the complex. How is the second molecule accommodated? In the accompanying paper (10), we show that the addition of either the cleavage domain alone or the *Fok*I–DNA-binding mutant *Fok*N13Y to the wild-type *Fok*I enzyme also can enhance the cleavage rate. However, both mutants restore wild-type cleavage levels only in high molar excess. This

suggests a requirement for DNA-binding by the second *Fok*I molecule. The second molecule may bind DNA nonspecifically on the same DNA molecule (cis binding) or bind specifically to a *Fok*I cognate site on another DNA molecule (trans binding). Because the Asn 13 to Tyr mutation in *Fok*N13Y is likely to affect only specific binding, we favor a model of dimerization of two *Fok*I molecules bound to two cognate sites (in trans) as the most efficient mechanism for cleavage at one site (Fig. 6). Although the requirement for the recognition of two sites is unusual in type II restriction endonucleases, it is not unprecedented. Activities of both *Eco*RII and *Sfi*I are stimulated by oligonucleotides containing their cognate sites. *Sfi*I exists as a tetramer, with each dimer recognizing a separate site (30). *Eco*RII may be more similar to *Fok*I in that it binds to two sites as a dimer (31). Overall, in more typical type II endonucleases such as *Bam*HI that bind and cleave at a single site, the function of dimerization is to mediate both recognition and cleavage. Our results from *Fok*I suggest that type IIs endonucleases have evolved a different cleavage mechanism in which recognition and cleavage are decoupled, with dimerization occurring after recognition as a way of regulating cleavage.

We thank the staff at Cornell High Energy Synchrotron Source and C. Escalante and L. Shen for help with data collection; L. Dorner and R. Kucera for protein purification; and T. Bestor, S. Halford, R. Roberts, and G. Wilson for helpful discussions. The work was supported by National Institutes of Health Grant GM44006 (A.K.A.) and National Eye Institute Training Grant 5T32EY07105 (D.A.W.).

1. Sugisaki, H. & Kanazawa, S. (1981) *Gene* **16,** 73–78.
2. Li, L., Wu, L. P. & Chandrasegaran, S. (1992) *Proc. Natl. Acad. Sci. USA* **89,** 4275–4279.
3. Kim, S. C., Podhajska, A. J. & Szybalski, W. (1988) *Science* **240,** 504–506.
4. Kim, Y.-G. & Chandrasegaran, S. (1994) *Proc. Natl. Acad. Sci. USA* **91,** 883–887.
5. Kim, Y.-G., Cha, J. & Chandrasegaran, S. (1996) *Proc. Natl. Acad. Sci. USA* **93,** 1156–1160.
6. Kim, Y.-G., Kim, P. S., Herbert, A. & Rich, A. (1997) *Proc. Natl. Acad. Sci. USA* **94,** 12875–9.
7. Kim, Y.-G., Shi, Y., Berg, J. M. & Chandrasegaran, S. (1997) *Gene* **203,** 43–49.
8. Wah, D. A., Hirsch, J. A., Dorner, L. F., Schildkraut, I. & Aggarwal, A. K. (1997) *Nature (London)* **388,** 97–100.
9. Schultz, S. C., Shields, G. C. & Steitz, T. A. (1991) *Science* **253,** 1001–1007.
10. Bitinaite, J., Wah, D. A., Aggarwal, A. K. & Schildkraut, I. (1998) *Proc. Natl. Acad. Sci. USA* **95,** 10570–10575.
11. Hirsch, J. A., Wah, D. A., Dorner, L. F., Schildkraut, I. & Aggarwal, A. K. (1997) *FEBS Lett.* **403,** 136–138.
12. Otwinowski, Z. & Minor, W. (1997) in *Macromolecular Crystallography, Part A,* eds. Carter, C. W. & Sweet, R. M. (Academic, San Diego), Vol. 276, pp. 307–326.
13. CCP4 (1994) *Acta Crystallogr. D* **50,** 760–763.
14. Navaza, J. & Saludjian, P. (1997) in *Macromolecular Crystallography, Part A,* eds. Carter, C. W. & Sweet, R. M. (Academic, San Diego), Vol. 276, pp. 581–594.
15. Jones, A. T., Zou, J. Y., Cowan, S. W. & Kjeldgaard, M. (1991) *Acta Crystallogr. A* **47,** 110–119.
16. Brunger, A. T. (1992) *X-PLOR*, *Ver. 3.1: A System for X-Ray Crystallography and NMR* (Yale Univ. Press, New Haven, CT).
17. Newman, M., Strzelecka, T., Dorner, L. F., Schildkraut, I. & Aggarwal, A. K. (1994) *Nature (London)* **368,** 660–664.
18. Winkler, F. K., Banner, D. W., Oefner, D., Tsernoglou, D., Brown, R. S., Heathman, S. P., Bryan, R. K., Martin, P. D., Petratos, K. & Wilson, K. S. (1993) *EMBO J.* **12,** 1781–1795.
19. Newman, M., Strzelecka, T., Dorner, L., Schildkraut, I. & Aggarwal, A. K. (1995) *Science* **269,** 656–663.
20. Wang, J. H., Yan, Y. W., Garrett, T. P., Liu, J. H., Rodgers, D. W., Garlick, R. L., Tarr, G. E., Husain, Y., Reinherz, E. L. & Harrison, S. C. (1990) *Nature (London)* **348,** 411–418.
21. Ryu, S. E., Kwong, P. D., Truneh, A., Porter, T. G., Arthos, J., Rosenberg, M., Dai, X. P., Xuong, N. H., Axel, R., Sweet, R. W., & Hendrickson, W. A. (1990) *Nature (London)* **348,** 419–426.
22. Waugh, D. S. & Sauer, R. T. (1994) *J. Biol. Chem.* **269,** 12298–12303.
23. Waugh, D. S. & Sauer, R. T. (1993) *Proc. Natl. Acad. Sci. USA* **90,** 9596–9600.
24. Hol, W. G. J. (1985) *Prog. Biophys. Mol. Biol.* **45,** 149–195.
25. Roberts, R. J. & Halford, S. E. (1993) in *Nucleases*, eds. Linn, S. M., Lloyd, R. S. & Roberts, R. J. (Cold Spring Harbor Lab. Press, Plainview, NY), 2nd Ed., pp. 35–88.
26. Kita, K., Kotani, H., Ohta, H., Yanase, H. & Kato, N. (1992) *Nucleic Acids Res.* **20,** 618.
27. Kita, K., Suisha, M., Kotani, H., Yanase, H. & Kato, N. (1992) *Nucleic Acids Res.* **20,** 4167–4172.
28. Li, L. & Chandrasegaran, S. (1993) *Proc. Natl. Acad. Sci. USA* **90,** 2764–2768.
29. Janin, J., Miller, S. & Chothia, C. (1988) *J. Mol. Biol.* **204,** 155–164.
30. Wentzell, L. M., Nobbs, T. J. & Halford, S. E. (1995) *J. Mol. Biol.* **248,** 581–595.
31. Kruger, D. H., Kupper, D., Meisel, A., Reuter, M. & Schroeder, C. (1995) *FEMS Microbiol. Rev.* **17,** 177–184.